

# **Light-induced Self-written Waveguides for Large Core Optical Fiber Modules**

Tatsuya Yamashita, Manabu Kagami

#### **Abstract**

A fabrication technique for producing lightinduced self-written (LISW) waveguides for large-core optical fibers is proposed. The proposed technique employs a photopolymerizable resin consisting of two kinds of photopolymerizable monomers that differ from each other in terms of both refractive index and polymerization mechanism. The core portion is formed by virtue of a self-trapping effect, in which visible light is irradiated to the resin through an optical fiber that is inserted into the resin. Only the low refractive index monomer can be radically polymerized to form the LISW waveguide, which is generated from one end of the fiber. After the irradiation is stopped, the concentration gradient induced by the

comsumption of the low refractive index monomer initiates a counter-diffusion phenomenon between the residual monomers. The low refractive index radically polymerizable monomer diffuses into the core region, while the high refractive index cationic polymerizable monomer diffuses out of the core region. The residual monomers are subsequently cured by exposure to UV light, and the region with decreased concentration of high refractive index monomer becomes a cladding layer. The resultant refractive index profiles of the waveguides were experimentally confirmed to be "W-shaped". The measured propagation loss of the waveguide was 1.7 dB/cm at 680 nm wavelength.

Keywords

Optical waveguide, Plastic optical fiber, Self-focusing, Photopolymerizable resin, Refractive index profile, Counter diffusion process

#### 1. Introduction

Optical wavelength division multiplexing (WDM) technology is now regarded as a promising approach for realizing high speed LANs for use in automobiles, because optical WDM communication can not only provide high-bandwidth, but also simplifies the sharing of several communication signals. For applications involving automobiles, reducing the system cost is the most important issue to address. However, conventional fabrication techniques for WDM modules are costly, because these techniques require the use of time-consuming processes such as the insertion of WDM filters. Therefore, in order to realize devices for high speed LANs for automobiles, it would be useful to develop a simple fabrication technique for WDM modules.

Attempts to simplify fabrication techniques for WDM modules have lead to an increasing interest in the use of Light-Induced Self-Written (LISW) waveguides. 2-10) When an optical fiber is adopted to irradiate a photopolymerizable resin, an optical waveguide can be produced automatically from the fiber by virtue of the self-trapping effect. 2, 3) Moreover, if WDM filters are arranged ahead of the fiber, it is also possible to form a waveguide that passes though the filters. Therefore, the use of LISW waveguides will probably serve to reduce the cost of WDM modules, because LISW waveguides enable us to eliminate the time-consuming process of inserting WDM filters into optical waveguide circuits.

So far, two types of fabrication techniques for LISW waveguides that also enable cladding layers to be formed by a photopolymerization process have been demonstrated. One of these involves the exchange of residual photopolymerizable resin surrounding the core region for another photopolymerizable resin with a lower refractive index after the core region has been produced by using the self-trapping effect. This technique (the cladding substitution LISW method) has a drawback in that it requires extra processes to exchange the resins. The other technique is based on a core region that is formed using a selective-photopolymerization process, in which only the higher refractive-index photopolymerizable monomer is polymerized and

the lower refractive index monomer is excepted from the polymerized portion in a photopolymerizable resin mixture that includes a higher refractive index photopolymerizable monomer and a lower refractive index photopolymerizable monomer.<sup>6, 9)</sup> By using the latter technique (the core selective-photopolymerization LISW method), the processes involved in the formation of the cladding layer can be greatly simplified when compared with the former technique. However, the latter technique is recognized as being impracticable for making large-core waveguides, because it takes a longer time to diffuse monomers over a longer distance. Therefore, in cases where we wish to use a largecore optical fiber (typically 500  $\sim$  1000  $\mu$ m in diameter), another technique that uses a simplified process is required.

Plastic optical fiber (POF) is considered to be the most suitable fiber for use in automobile applications, because it can offer low connection costs and robustness for tight bends due to its large core size and high numerical apertures (NA). A WDM module for POF was able to be produced by the cladding substitution LISW method, and the feasibility of using a WDM module for automobile applications has been reported. In this report, a novel selective-photopolymerization LISW method is proposed in order to reduce the process cost of producing WDM modules for POF.

## 2. Proposed LISW waveguide for an optical fiber with a large core

The proposed fabrication processes for forming LISW waveguides for large-core optical fibers are shown schematically in **Fig. 1**. The photopolymerizable resin used in this technique includes two kinds of photopolymerizable monomers,  $\mathbf{A_m}$  and  $\mathbf{B_m}$ . Monomer  $\mathbf{A_m}$  can be polymerized by irradiating with light at a wavelength shorter than  $\lambda_a$  to form polymer  $\mathbf{A_p}$ , and monomer  $\mathbf{B_m}$  can be polymerized by irradiating with light at a wavelength shorter than  $\lambda_b$  to form polymer  $\mathbf{B_p}$ . The wavelength  $\lambda_a$  must be longer than  $\lambda_b$ , and the refractive index of polymer  $\mathbf{A_p}$  must be lower than that of polymer  $\mathbf{B_p}$ . In the first stage, a core region is created in the photopolymerizable resin by using the self-trapping effect of a light beam (Fig. 1(b)). An optical fiber is

introduced into the resin and delivers a light beam at wavelength  $\lambda_w$ , which is somewhere between  $\lambda_a$  and  $\lambda_b$ . This light beam can therefore only induce polymerization of monomer  $A_m$ . If the optical fiber has a large core size, then the area where photopolymerization occurs is too large for monomer  $B_m$  to diffuse out of the polymerized region. Thus, the core region created in this stage is composed of both polymer  $A_p$  and monomer  $B_m$ . In the second stage, a layer that is deficient in concentration of monomer  $B_m$  is formed by the counter-diffusion of monomers  $\boldsymbol{A}_{m}$  and  $\boldsymbol{B}_{m}$ , as follows. Monomer  $A_m$  diffuses into the core region that was created in the first stage in order to reduce the concentration gradient of monomer  $A_m$ . This diffusion of monomer  $A_m$  causes the unreacted molecules of monomer  $B_m$  that remain in the core region to diffuse out of the core. As a result, a layer that is deficient in concentration of monomer  $B_m$  is produced around the surface of the core region (Fig. 1(c)). In the final stage, the residual monomers are polymerized by irradiating with a light at a wavelength  $\lambda_c$ , which is shorter than  $\lambda_b$ , as shown in Fig. 1(d). The layer that was produced in the second stage becomes a cladding layer after polymerization in the final stage, because the concentration of polymer  $\mathbf{B}_{\mathbf{n}}$  in the layer is lower than that in the core region. The refractive index of the resultant waveguide exhibits a W-shaped profile.

#### 3. Experimental methods

## 3.1 Material

The photopolymerizable resin used in this report was a mixture of radical and cationic polymerizable monomers, including photoinitiators for the monomers. The photoinitiator used for the radical

polymerization was selected to be sensitive to light at a wavelength of 488 nm, while the photoinitiator for the cationic polymerization was insensitive to light at this wavelength but was sensitive to light from a high-pressure mercury lamp. Ethoxylated trimethylolpropane triacrylate was used for monomer  $A_m$ , which has a refractive index of 1.469. This is a radical polymerizable monomer that forms polymer  $A_p$ , which has a refractive index

of 1.490. The diglycidyl ether of bisphenol A was used as monomer  $\mathbf{B}_{\mathbf{m}}$ , which has a refractive index of 1.569. This is a cationic polymerizable monomer that forms polymer  $\mathbf{B}_{\mathbf{p}}$ , which has a refractive index of 1.590. The weight ratio of monomer  $\mathbf{A}_{\mathbf{m}}$  to monomer  $\mathbf{B}_{\mathbf{m}}$  was 0.6:0.4. The refractive index of the photopolymerizable resin  $(n_{Cm})$  was 1.509, and that of the polymerized resin  $(n_{Cp})$  was 1.536.

## 3. 2 Formation of the LISW waveguides

The experimental set-up used to fabricate the LISW waveguides is shown in **Fig. 2**. A quasi graded-index type POF with a 700  $\mu$ m core diameter, a 750  $\mu$ m cladding diameter and an NA of 0.25 (Eska-Miu, supplied by Mitsubishi Rayon Co., Ltd., Japan) was used in this experiment. The photopolymerizable resin was introduced into a transparent cell and one end of a POF was immersed

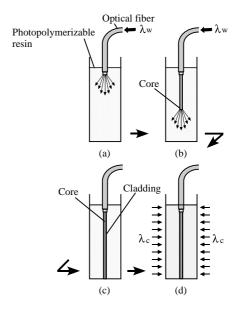


**Fig. 1** Fabrication processes to produce LISW waveguides for use with large-core optical fibers.

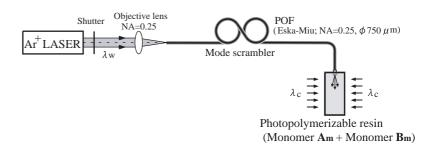


**Fig. 2** Schematic diagram of the experimental set-up used for fabrication of the LISW waveguides.

into the resin. A continuous-wave beam from an argon-ion laser ( $\lambda_w = 488 \text{ nm}$ ) was focused onto the other end of the POF by means of an objective lens with an NA of 0.25. The photopolymerizable resin was irradiated by the continuous-wave beam that was radiated from the immersed end of the POF, and the irradiation power P was measured at the end. The duration of the irradiation was denoted as  $t_1$ . After the irradiation was terminated, the resin was kept in a dark place for a set time  $t_x$  to allow diffusion to take place. The resin was finally uniformly exposed to UV light from a 200 Watt high-pressure mercury lamp. All of these experiments were carried out under atmosphere at room temperature.

#### 3. 3 Analysis of refractive index profiles

The refractive index profiles were analyzed using a transmitted dual-beam interference microscope. In order to evaluate the refractive index profiles of the fabricated LISW waveguides, slices of waveguide were used that had been cut along the core section with a diamond saw. In cases where we wanted to evaluate changes in the refractive index profiles with time, two-dimensional samples corresponding to cross-sections of the LISW waveguides were prepared using the set-up shown in Fig. 3, as follows. The photopolymerizable resin was sandwiched between two transparent glass plates of 0.15 mm thickness. The thickness of the resin layer was adjusted by using a spacer plate with a thickness of 0.15-0.16 mm. One end of the optical fiber, which had a core diameter of 600  $\mu m$  and an NA of 0.37, was then contacted onto the top of the glass plate, and light at a wavelength of 488 nm was used to irradiate the photopolymerizable resin from the end of the optical fiber via the glass plate to form the core. The refractive index profile of the two-

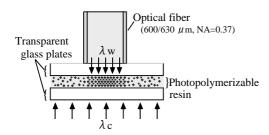
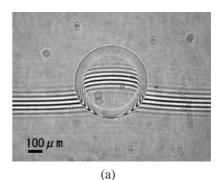


**Fig. 3** Experimental set-up used to investigate refractive index changes induced by photopolymerization.

dimensional sample between the glass plates was able to be observed, even if photopolymerizable monomers still remained in the sample. The maximum refractive index difference between the core region and the cladding layer is denoted as  $\Delta n_m$  (see **Fig. 5**(b)). The core diameter is defined as the distance between the positions that have the lowest refractive indices, and is denoted as  $d_w$  (see Fig. 5(b)).

#### 3. 4 Measurement of optical properties

An LISW optical waveguide sample that was prepared under the following conditions; P = 80 mW,  $t_1 = 150$  sec and  $t_x = 5$  min, was used to measure the optical properties. The propagation loss of the waveguide was measured by the cutback method, as follows. Light from a white lamp source was coupled into a pigtailed fiber, which was used for forming the core region of the LISW waveguide. Then, the outgoing light from a certain length of the cut waveguide was coupled into a multimode fiber with a core diameter of  $1000 \, \mu \text{m}$  and an NA of 0.38. The optical power from the output end of the fiber



1.55*n*1.54

1.53

1.52

1.52

1.51

1.50

1.50

1.51

1.50

1.50

1.50

1.50

1.50

1.50

1.50

1.50

1.50

1.50

1.50

1.50

1.50

1.50

1.50

1.50

1.50

1.50

1.50

1.50

1.50

1.50

1.50

1.50

1.50

1.50

1.50

1.50

1.50

1.50

1.50

1.50

1.50

1.50

1.50

1.50

1.50

1.50

1.50

1.50

1.50

1.50

1.50

1.50

1.50

1.50

1.50

1.50

1.50

1.50

1.50

1.50

1.50

1.50

1.50

1.50

1.50

1.50

1.50

1.50

1.50

1.50

1.50

1.50

1.50

1.50

1.50

1.50

1.50

1.50

1.50

1.50

1.50

1.50

1.50

1.50

1.50

1.50

1.50

1.50

1.50

1.50

1.50

1.50

1.50

1.50

1.50

1.50

1.50

1.50

1.50

1.50

1.50

1.50

1.50

1.50

1.50

1.50

1.50

1.50

1.50

1.50

1.50

1.50

1.50

1.50

1.50

1.50

1.50

1.50

1.50

1.50

1.50

1.50

1.50

1.50

1.50

1.50

1.50

1.50

1.50

1.50

1.50

1.50

1.50

1.50

1.50

1.50

1.50

1.50

1.50

1.50

1.50

1.50

1.50

1.50

1.50

1.50

1.50

1.50

1.50

1.50

1.50

1.50

1.50

1.50

1.50

1.50

1.50

1.50

1.50

1.50

1.50

1.50

1.50

1.50

1.50

1.50

1.50

1.50

1.50

1.50

1.50

1.50

1.50

1.50

1.50

1.50

1.50

1.50

1.50

1.50

1.50

1.50

1.50

1.50

1.50

1.50

1.50

1.50

1.50

1.50

1.50

1.50

1.50

1.50

1.50

1.50

1.50

1.50

1.50

1.50

1.50

1.50

1.50

1.50

1.50

1.50

1.50

1.50

1.50

1.50

1.50

1.50

1.50

1.50

1.50

1.50

1.50

1.50

1.50

1.50

1.50

1.50

1.50

1.50

1.50

1.50

1.50

1.50

1.50

1.50

1.50

1.50

1.50

1.50

1.50

1.50

1.50

1.50

1.50

1.50

1.50

1.50

1.50

1.50

1.50

1.50

1.50

1.50

1.50

1.50

1.50

1.50

1.50

1.50

1.50

1.50

1.50

1.50

1.50

1.50

1.50

1.50

1.50

1.50

1.50

1.50

1.50

1.50

1.50

1.50

1.50

1.50

1.50

1.50

1.50

1.50

1.50

1.50

1.50

1.50

1.50

1.50

1.50

1.50

1.50

1.50

1.50

1.50

1.50

1.50

1.50

1.50

1.50

1.50

1.50

1.50

1.50

1.50

1.50

1.50

1.50

1.50

1.50

1.50

1.50

1.50

1.50

1.50

1.50

1.50

1.50

1.50

1.50

1.50

1.50

1.50

1.50

1.50

1.50

1.50

1.50

1.50

1.50

1.50

1.50

1.50

1.50

1.50

1.50

1.50

1.50

1.50

1.50

1.50

1.50

1.50

1.50

1.50

1.50

1.5

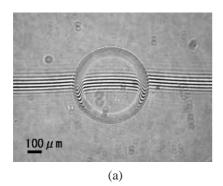
**Fig. 4** Refractive index profile before UV exposure. (a) Interferogram obtained by interference microscopy, (b) calculated refractive index profile.

was measured using an optical power meter. The propagation loss was obtained from the slope of the graph of the insertion loss versus the waveguide length L. The coupling loss was estimated as the insertion loss at L=0 mm.

#### 4. Experimental results and discussion

### 4. 1 Change of refractive index profiles

**Figure 4**(a) shows a typical interferogram of a two-dimensional sample fabricated under the following conditions; P = 30 mW,  $t_1 = 20$  sec,  $t_x = 60$  sec. The estimated refractive index profile is also depicted in Fig. 4(b). The photopolymerized region that was induced by the irradiation from the optical fiber was identified from increases in the refractive index. At the surface of the photopolymerized region, a decrease in the refractive index was observed. Although the refractive index was increased over the whole area of the sample by the subsequent UV exposure ( $\sim 1.6$  mJ), the position where the minimum refractive index was observed remained unchanged, as shown in Fig. 5. **Figure 6** 



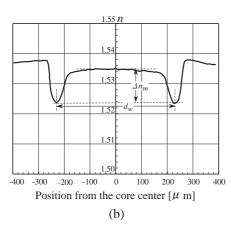


**Fig. 5** Refractive index profile after UV exposure. (a) Interferogram obtained by interference microscopy, (b) calculated refractive index profile.

shows the changes of the maximum refractive index difference  $\Delta n_m$  and the core diameter  $d_w$  as a function of the diffusion time  $t_x$ . The conditions to prepare the sample were as follows, P=30 mW,  $t_1=30$  sec. As shown in Fig. 6(a), the value of  $\Delta n_m$  increased rapidly as  $t_x$  increased, and exhibited a tendency to saturate above approximately  $t_x>10$  min. The value of  $d_w$  decreased slightly, as shown in Fig. 6(b). These results support that mechanism that counter-diffusion of monomers through the core/cladding interface occurs after irradiation from the fiber has terminated, whereby the low refractive index monomer  $A_m$  moves into the core region and the high refractive index monomer  $B_m$  moves toward the outer portion of the core region.

Next, the uniformity of the refractive index profile along the LISW waveguide was investigated. A waveguide sample fabricated under the following

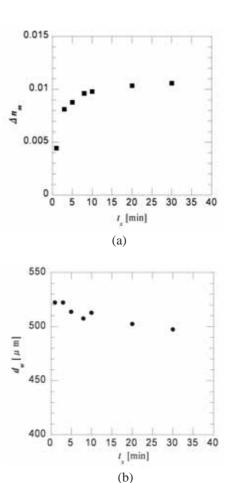
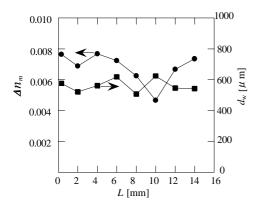


**Fig. 6** Changes in the maximum refractive index difference  $\Delta n_m$  (a) and the core diameter  $d_w$  (b) against the diffusion time  $t_x$ , observed after UV exposure.

conditions; P = 80 mW,  $t_1 = 300$  sec and  $t_x = 5$  min, was used in this investigation. **Figure 7** shows the dependence of the maximum refractive index difference  $\Delta n_m$  and the diameter  $d_w$  on the distance from the fiber tip. The values of  $\Delta n_m$  and  $d_w$  were found to vary with waveguide position, and the minimum relative refractive index difference was estimated at 0.52 % (corresponding to an NA of 0.15). These results suggest that this waveguide could show a significant level of radiation loss.

## 4. 2 Optical properties

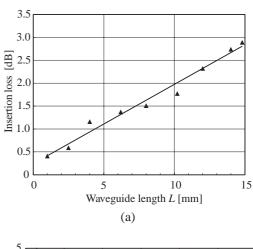
Figure 8(a) shows the insertion loss as a function of waveguide length L at a wavelength of 680 nm. The coupling loss and the propagation loss at this wavelength were estimated to be 0.25 dB and 1.7 dB/cm, respectively. A rapid increase was observed in the propagation loss spectrum in the shorter wavelength region, below 600 nm (Fig. 8(b)). As observed in Fig. 7, it is possible that the radiation loss arises from both an insufficient difference in refractive index and non-uniformity of the core diameter. In addition, some scattering loss seems to be induced because the photopolymerized resin was slightly cloudy after the UV exposure. Therefore, the propagation loss is considered to include components of both radiation loss and scattering loss. It is supposed that these problems could be solved by means of both the selection of appropriate materials and the correct fabrication conditions.



**Fig. 7** The dependence of the maximum refractive index difference  $\Delta n_m$  and the core diameter  $d_w$  on the distance from the fiber tip.

#### 5. Conclusion

A novel technique for forming large-core LISW waveguides is proposed. A "W-shaped" refractive index profile was successfully realized. The origin of this form of profile can be explained by a counter-diffusion phenomenon of the monomers. At present, there is a remarkable scattering loss in the shorter wavelength region and a propagation loss of 1.7 dB/cm at a wavelength of 680 nm. If these optical properties could be improved by means of both appropriate material selection and better fabrication conditions, this technique could be used to produce low-cost WDM modules for large-core optical fibers, and these might be expected to encourage an expansion in the use of high speed LANs for automobiles.



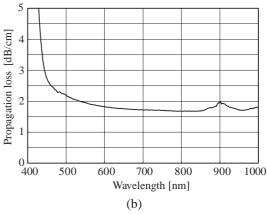


Fig. 8 Loss properties of an LISW optical waveguide measured by a cutback method.

(a) Insertion loss as a function of waveguide length, (b) Propagation loss spectrum.

#### References

- Kagami, M.: "Visible Optical Fiber Communication", R&D Rev. of Toyota CRDL, 40-2(2005), 1
- 2) Frisken, S. J.: "Light-induced Optical Waveguide Uptapers", Opt. Lett., **18**-3(1993), 1035
- 3) Kewitsch, A. S. and Yariv, A.: "Self-focusing and Self-trapping of Optical Beams upon Photopolymerization," Opt. Lett., **21**-1(1996), 24
- 4) Monro, T. M., de Sterke, C. M. and Poladian, L.: "Self-writing a Waveguide in Glass using Photosensitivity", Opt. Commun., **119**(1996), 523
- 5) Maruo, S. and Kawata, S.: "Optically-induced Growth of Fiber Patterns into a Photopolymer", Appl. Phys. Lett., **75**-5(1999), 737
- Kagami, M., Yamashita, T. and Ito, H.: "Lightinduced Self-written Waveguide Three-dimensional Optical Waveguide", Appl. Phys. Lett., 79-8(2001), 1079
- 7) Yoshimura, T., Ojima, M., Arai, Y. and Asama, K.:
  "Three-dimensional Self-organized
  Microoptelectronic Systems for Board-level
  Reconfigurable Optical Interconnects Performance
  Modeling and Simulation", IEEE J. Select. Topics
  Quantum Electron., 9-2(2003), 492
- 8) Watanabe, N., Murata, Y., Oyama, Y., Ito, T., Ozawa, H., Mikami, O. and Shioda, T.: "Self-written Connection between GI-MMF and VCSEL Using Green Laser", IEICE Trans. Electron., **J87-C**(2004), 488
- 9) Yamashita, T., Kagami, M. and Ito, H.: "Waveguide Shape Control and Loss Properties of Light-induced Self-written (LISW) Optical Waveguides", J. Lightwave Technol., **20**-8(2002), 1156
- 10) Yamashita, K., Hashimoto, T., Oe, K., Mune, K., Naitou, R. and Mochizuki, A.: "Self-written Waveguide Structure in Photosensitive Polyimide Resin Fabricated by Exposure and Thermosetting Process", IEEE Photo. Tech. Lett., 16-3(2004), 801

- 11) Dorkenoo, K., Cregut, O., Mager, L., Gillot, F., Carre, C. and Fort, A.: "Quasi-solitonic Behavior of Self-written Waveguides Created by Photopolymerization", Opt. Lett., **27**-20(2002), 1782
- 12) Sugihara, O., Tsuchie, H., Endo, H., Okamoto, N., Yamashita, T., Kagami, M. and Kaino, T.: "Light-induced Self-written Polymeric Optical Waveguides for Single-mode Propagation for Optical Interconnections", IEEE Photo. Tech. Lett., 16-3(2004), 804
- 13) Yonemura, M.: "250 Mbit/s Bi-directional Single Plastic Optical Fiber Communication Systems", R&D Rev. of Toyota CRDL, **40**-2(2005), 18

(Report received on May 9, 2005)



#### Tatsuya Yamashita

Research Field : Guided-wave optical devices, Polymer-based optical components

Academic society: Inst. Electron., Inf. Commun. Eng., Jpn. Soc. Appl. Phys., Opt. Soc. Jpn., Opt. Soc. Am.



#### Manabu Kagami

Research Field : Optical communication devices

Academic degree: Dr. Eng.
Academic society: Inst. Electron., Inf.
Commun. Eng., Inst. Electr.
Electron. Eng., Opt. Soc. Am.,
Jpn. Soc. Appl. Phys., Jpn. Inst.
Electron. Packag.